# Underestimation of Anthropogenic Bromoform Released into the Environment?

Etienne Quivet, Patrick Höhener, Brice Temime-Roussel, Julien Dron, Gautier Revenko, Maxime Verlande, Karine Lebaron, Carine Demelas, Laurent Vassalo, Jean-Luc Boudenne

# Underestimation of anthropogenic bromoform released into the environment?

Etienne Quivet[a], Patrick Höhener[a], Brice Temime-Roussel[a], Julien Dron[b], Gautier Revenko[b], Maxime Verlande[a], Karine Lebaron[a], Carine Demelas[a], Laurent Vassalo[a], Jean-Luc Boudenne[a],*

[a] Aix Marseille Univ, CNRS, LCE, 3 place Victor Hugo 13003 Marseille, France
[b] Institut écocitoyen pour la connaissance des pollutions, Centre de vie de la Fossette, RD 2668, 13270 Fos-sur-Mer, France

Corresponding author:
Jean-Luc Boudenne, Aix-Marseille University, CNRS, Faculty of Sciences, Department of Chemistry, Laboratory of Environmental Chemistry, 3 place Victor Hugo - case 29, 13331 Marseille cedex 3, France, jean-luc.boudenne@univ-amu.fr, Phone : +33413551031

## Graphical abstract

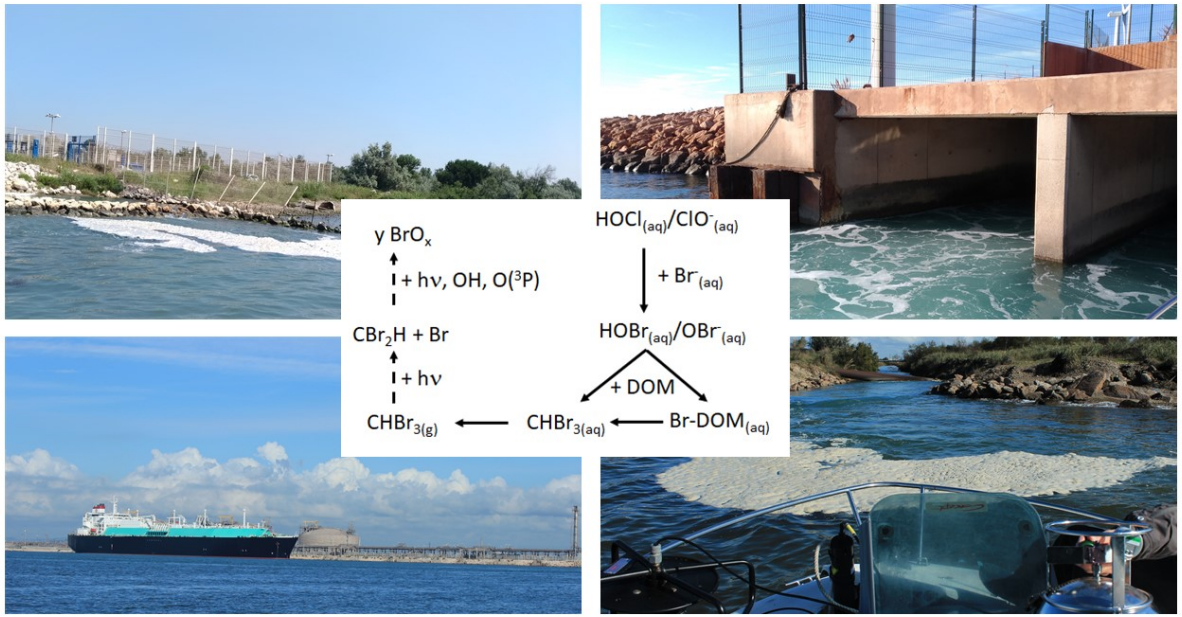


**Abstract**

Bromoform ($CHBr_3$) belongs to very-short-lived substances (VSLSs), which are important precursors of reactive bromine species (BrOx) contributing to tropospheric and stratospheric chemistry. To date, most models calculating bromine product emissions to the atmosphere only consider the natural production of $CHBr_3$ from marine organisms such as macroalgae and phytoplankton. However, $CHBr_3$ has many other anthropogenic sources (coastal industrial sites, desalination and wastewater plants, ballast waters, and seawater toilets) that may drastically increase the amounts emitted in the atmosphere. Here, we report the levels of $CHBr_3$ released in water and air (according to real-time and offline measurements by proton-transfer-reaction time-of-flight mass spectrometry (PTR-ToF-MS) and gas chromatography with electron capture detection (GC-ECD)) in a highly industrialized area where 3 million cubic meters of chlorinated seawater is released each day, which were

measured during six field campaigns (at sea and on land) distributed over three years. The highest levels found during this survey (which were correlated to the physical-chemical characteristics of the water, meteorological and hydrological conditions, salinity, and temperature gradients along the water column) reached 34.6 μg $L^{-1}$ in water (100-10,000 times higher than reported natural levels) and 3.9 ppbv in the air (100 times higher than the maximum reported value to date). These findings suggest the need to undertake sampling and analysis campaigns as close as possible to chlorinated discharges, as anthropogenic $CHBr_3$ sources from industrial discharges may be a missing factor in global flux estimates or organic bromine to the atmosphere.

**Keywords:** Disinfection By-products; Electrochlorination; Atmosphere; Proton Transfer Reaction Time-of-flight Mass Spectrometry; Modeling

## Introduction

Bromoform ($CHBr_3$) is one of the most important halogenated very short-lived substances (VSLSs) that affect tropospheric chemistry.[1,2] It is naturally formed in seawater by various marine organisms at a broad range of trophic levels, including invertebrates, algae,[3-5] seagrass,[6] bacteria[7], virus[8], and zooplankton.[9] Bromoperoxidases, located at or near the surface of such organisms, oxidize $Br^-$ (naturally occurring in seawater at levels of approximatively 65 mg $L^{-1}$) in the presence of $H_2O_2$ into HOBr, which in turn reacts with natural dissolved organic matter (DOM) to form $CHBr_3$ and other brominated compounds.[10,11] The sea-to-air flux originating from these biogenic sources is estimated to range between 3 and 22 Gmol Br $year^{-1}$, with "hot spots" of $CHBr_3$ emissions in coastal and oceanic upwelling regions,[1,12,13] and in the tropical Indian Ocean and subtropical northern Atlantic.[2,14] These estimates are bounded by a high degree of uncertainty due to the spatiotemporal variability of VSLS emissions, which are driven by changes in sea surface temperature and meteorology, and primary productivity, biogeochemical cycling.[14,15]

Another important source of $CHBr_3$ emissions is linked to the chlorination of seawater. This process is considered one of the most effective means of controlling biofilm formation (microfouling), which may block heat exchangers or cause the development of molds (macrofouling) in industrial pipelines. Chlorination is used at many industrial sites around the world that use the "disinfected" water for cooling purposes (petrochemical and steel industry facilities and nuclear and thermal power plants),[16] warming purposes (liquefied natural gas (LNG) terminals for

the gasification of liquids),[17,18] or production of drinking water (desalination plants).[19,20] This process has also been selected by the International Maritime Organization as one of the *best available technologies* for the control and management of ballast water from ships before discharge into the sea.[21] Moreover, several coastal cities around the world that use seawater for toilet flushing chlorinate their wastewater effluents before discharge into the sea.[22] Regarding biogenic sources, the presence of $CHBr_3$ in such effluents is linked to the rapid conversion of $HOCl/OCl^-$ into $HOBr/OBr^-$ in bromide-rich waters ($k = 1.55 \times 10^3\ M^{-1}\ s^{-1}$),[23] followed by the reaction of $HOBr/OBr^-$ with DOM.[24] The amount of $CHBr_3$ produced industrially is not well known as atmospheric measurements are not able to distinguish natural from anthropogenic $CHBr_3$ sources, making it difficult to measure large-scale $CHBr_3$ emissions from chlorinated waters. However, based on reported $CHBr_3$ levels between 0.5 and 50 $\mu g\ L^{-1}$ in cooling waters, Chipperfield et al.[2] estimated that anthropogenic emissions of $CHBr_3$ in southeast Asia could reach a level 30%higher than the measurement-based estimates of total emissions derived for the same region.[2] Similarly, simulations with the Lagrangian particle dispersion model FLEXPART conducted by Maas et al. showed mean anthropogenic $CHBr_3$ mixing ratios 2 to 6 times higher than the climatological $CHBr_3$ estimate in coastal waters of East Asia.[25]

Once naturally or anthropogenically formed in seawater, $CHBr_3$ may have direct harmful impacts on marine organisms,[26-28] but its impact on atmospheric chemistry is of greater concern. Once in the marine boundary layer a large fraction of $CHBr_3$ is transferred to the atmosphere (the dimensionless Henry's law constant ranges between 0.0063 at 0 °C and 0.0217 at 20 °C in seawater with a salinity of 30.4),[29] where it is either photolyzed in the atmosphere into bromine radicals or reacts with hydroxyl radicals to form reactive bromine species.[3] These bromine species affect ozone and mercury in both the upper-troposphere and the lower stratospheric region.[30-33] In regions of deep convection (such as the tropics near the equator) and in summer monsoon regions (such as Southeast Asia), VSLSs may be entrained directly into the stratosphere where they contribute to ozone layer depletion at middle and high latitudes.[1,25,33,34] $CHBr_3$ is also involved in particle formation and may control the formation of cloud condensation nuclei, giving it a significant role in climate change.[5,12] Current estimates of $CHBr_3$ emissions are generally simulated either by a top-down approach (using surface ocean and atmospheric measurements), or, more often, by a bottom-up approach (i.e, by measuring $CHBr_3$ levels in air and seawater -during ship cruises- and then simulating their atmospheric mixing ratios by calculating the sea-to-air fluxes).[12,14,35] Top-down $CHBr_3$ emission estimates are generally 2-fold larger than bottom-up estimates;[25] the large spatiotemporal variability of $CHBr_3$ in surface water and air, combined with poor temporal and spatial data coverages, may explain the large deviations between these two methods of estimation.[25,36] Recent papers have also highlighted the low levels of knowledge on anthropogenic $CHBr_3$ released in the

atmosphere, and when taken into account, anthropogenic $CHBr_3$ levels in air are often linked to the concentration in water and then derived by sea-to-air flux models.[1,2,25,36]

The present paper presents for the first time the anthropogenic $CHBr_3$ emitted from various industrial plants (steel and (petro)chemical plants and LNG terminals) both in water and in air. This three year survey was conducted in a heavily industrialized area (Gulf of Fos, Mediterranean Sea) where more than 3 million cubic meters of chlorinated seawater is released each day and include both real-time and offline measurements. Modeling of $CHBr_3$ transfer from water to air demonstrates that these fluxes may reach 16.1 mg $m^{-2}$ $day^{-1}$, as compared to calculated natural $CHBr_3$ sea-to-air flux of 0.024 to 2.58 mg $m^{-2}$ $day^{-1}$ for the shore and 0.006 to 0.24 mg $m^{-2}$ $day^{-1}$ for the shelf regimes.[1]

## Materials and methods

### *Study site and sampling sites description*

The Gulf of Fos is a semi-enclosed bay covering 42 $km^2$ and having a mean depth of 8 m, although there is a navigation channel in its central part with a 24 m depth and 200 m width, [37], which was dug to allow LNG and oil tankers, container ships and other deep-draft vessels to dock at industrial terminals. This bay is located in the Gulf of Lion (northwestern Mediterranean Sea) between the mouth of the Rhône River to the west, the Berre lagoon to the northeast and the city of Marseille to the southeast (Figure 1). Two main wind regimes occur in this bay: i) a north and northwestern wind ("Mistral"), which brings cold and dry air (approximatively 40% per year) and is also responsible for coastal upwelling in the Gulf,[38] and ii) a southeasterly wind (10- 20% per year), which can induce high wave breaking close to the seashore. The mean tidal range is approximatively 20 cm, and the associated currents are extremely low.

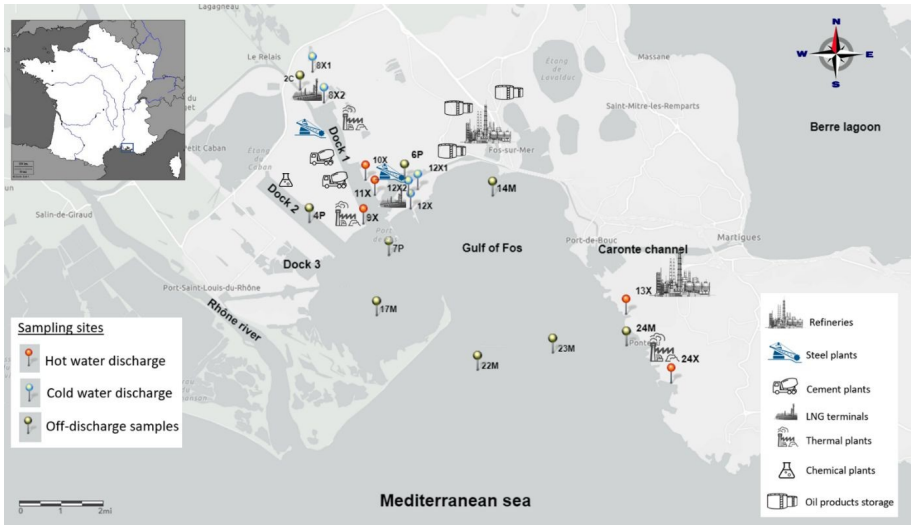

*Figure 1. Sampling sites located throughout the Gulf of Fos, France. Sampling points located at industrial outlets are represented in orange (hot discharges) and blue (cold discharges). Samples taken outside the discharges are represented in yellow.*

The Gulf receives several freshwater inputs, including the main input from the Rhône River (approximatively1,700 $m^3$ $s^{-1}$), whose plume may enter the Gulf under southeastern wind conditions and minor inputs from the Berre lagoon (releasing brackish water from the east through the Caronte channel at approximatively 260 $m^3$ $s^{-1}$), and irrigation and navigation canals flushing into Dock #1 (approximatively 50 $m^3$ $s^{-1}$).[39]

The Gulf of Fos hosts the most important industrial harbor in France and the Mediterranean Sea, which has various heavy industrial activities (Figure 1), the majority of which use chlorinated seawater for cooling or heating purposes. Two large LNG terminals discharge chlorinated waters at 7,500 $m^3$ $h^{-1}$ (8X) and 16,000 $m^3$ $h^{-1}$ (12X). These releases will be henceforth called "cold discharges" (the outlet temperature is lower than the inlet temperature). Atmospheric and water samples were collected both at the open rack vaporizers (ORV) (12X1), which are vaporizers in which LNG flowing inside a heat-transfer tube exchanges heat with seawater flowing outside the heat-transfer tube to gasify the LNG, and near the site's outlet (12X2). 12X2 was dedicated to online and real-time measurements of atmospheric $CHBr_3$, and 12X was dedicated to water sampling. At 8X, chlorinated seawater is discharged either into a canal located northeast of the LNG plant (8X1) or directly into the Gulf, southeast of the LNG plant (8X2).

A steel plant (11X) and oil refinery (13X) also discharge chlorinated seawater at flows exceeding 20,000 $m^3$ $h^{-1}$. Three gas power plants (9X, 10X, and 24X) intermittently chlorinate seawater at levels reaching 24,000 $m^3$ $h^{-1}$, 17,000 $m^3$ $h^{-1}$, and 32,000 $m^3$ $h^{-1}$, respectively. The steel, petrochemical, and power plant releases will be henceforth called "hot water discharges" (the outlet temperature is higher than the inlet temperature).

In Europe, seawater chlorination is carried out for 6-9 months of a year (from spring to fall)[16]
as a function of industrial activities and water temperature (the temperature must exceed approximatively 10 °C as micro- and macrofouling are more pronounced in warm water conditions).[40] The applied chlorine dose depends on the oxidant demand of the water and of the circuits; the dose is in the range of 0.5-1.5 mg $L^{-1}$ in the case of a low-level chlorination process or greater than or equal to 2 mg $L^{-1}$ $Cl_2$ in the case of shock chlorination.[16]

Supplementary sampling was performed at one of the freshwater inlet channels in the Gulf (i.e., the shipping canal from Arles to Port-de-Bouc

(2C)), two of the harbor basins located to the north of the gulf (4P and 6P), and six points spread across the Gulf from the coves (17M, 7P and 14M) to the open sea (22M, 23M and 24M).

***Water and air sampling***

Air and water sampling took place during six field campaigns from Apr. 2017 to June 2019 at stations located at sea and on land, as summarized in Table S1 and presented in Figure 1.

Air sampling was performed according to two modes, either by the use of canisters (at-sea, grab and instantaneous samples) or by the use of a sampling pole installed on the roof of a laboratory truck (on-land sampling at station 12X2), which was connected directly to a proton-transfer-reaction time-of-flight mass spectrometry (PTR-ToF-MS) analyzer (see section 2.3). This second mode of sampling allowed online and continuous sampling (at approximatively 2 m above the ground) and real-time measurements (3.5 min temporal resolution) of $CHBr_3$ in air.

Canister air samples were taken at a height of less than one meter above the water surface concurrently with the water samples. Instantaneous air samples were drawn into cleaned and pre-evacuated 6-L silonite-treated canisters (Entech Instruments, Inc.). Analysis was carried out within 24 hours after sampling to minimize any potential compound losses due to canister storage. Laboratory tests, where a canister filled with an air sample containing $CHBr_3$ was analyzed between 6 hours and 7 days after sampling, showed that the sample integrity could be maintained over this period, as no significant loss was observed.

Moreover, to estimate the sampling contamination induced by laboratory pollution, sample handling, and storage, air blanks were regularly carried out. No $CHBr_3$ contamination was detected.

Water samples were collected, at the surface and at a depth of è m (or 1 m above the seabed when above 7 m) by use of a 5-L Niskin bottle (General Oceanics, USA) and divided into 1-L amber glass bottles: one bottle contained ascorbic acid (5 mL, 120 g $L^{-1}$) as a quenching reagent preventing any residual chlorine reaction for further analysis of $CHBr_3$, and another bottle contained no preservative for further analysis of nonpurgeable organic carbon (NPOC), ammonium ($NH_4^+$), total nitrogen (TN), $NO_3^-$, $Cl^-$, $Br^-$ and $SO_4^{2-}$. All the samples were then stored at 4 °C in the dark until analysis in the laboratory. Temperature, pH, and salinity were recorded throughout the water column during water sampling by use of a CTD-type multiparameter probe (MS5, OTT Hydrolab, Germany). The flow velocity at each sampling point exceeding 3 m depth was measured by an acoustic Doppler current profiler (ADCP) current meter (Aquadopp 600 kHz profiler, Nortek) along a vertical profile with measured points averaged over 1 m cells. The water quality parameters are summarized in Table S2.

***Air analysis by PTR-ToF-MS***

A PTR-ToF 8000 mass analyzer (PTR-ToF-MS 8000, Ionicon Analytik GmbH, Innsbruck, Austria) was deployed to measure $CHBr_3$ concentration i) in continuous mode (12X2) and ii) in offline mode after canister sampling at other sampling sites. Analysis was performed using $O_2^+$ as the primary reagent ion to allow the detection of halogenated hydrocarbons not ionizable via proton transfer. The reaction chamber pressure (pdrift) was 2.20 mbar, the drift tube voltage was 543 V, and the drift tube temperature was held constant at 333 K. The corresponding E/N ratio was 134 Td (1Td = 10-17 V $cm^2$), where E is the electric field strength applied to the drift tube and N is the buffer gas density. Data from PTR-ToF-MS were analyzed with Tofware software (v 2.5.7, Tofwerk).

The sensitivity of the instrument for $CHBr_3$ detection was experimentally assessed using a permeation device consisting of a homemade permeation tube containing 500 mg of liquid CHBr3 (amylene stabilized, analytical standard, Sigma-Aldrich) and a permeation unit (PUL 200, Calibrage). The permeation cell was kept at a constant temperature (60 °C) under a controlled flow of nitrogen (100 mL $min^{-1}$). Under these conditions, the gravimetrically determined generation of $CHBr_3$ was 11.1 ± 0.4 mg $h^{-1}$. To reach the working concentration range of the instrument, an additional dilution step was added at the outlet of the permeation device, using a controlled flow of nitrogen (0-1 L $min^{-1}$). Calibration was performed with 7 concentrations repeated twice.

Reactions between halogenated volatile organic compounds (VOCs) and $O_2^+$ as the reagent ion have been reported to proceed via a dissociative charge transfer reaction, generally resulting in the loss of a halogenated atom.[41] In the case of halogenated VOCs containing both bromine and chlorine atoms, the loss of a bromine atom is favored.[42] A preliminary study that consisted of an analysis of gaseous $CHBr_3$ and chlorodibromomethane ($CHBr_2Cl$, 97%, Sigma-Aldrich) by PTR-ToF-MS validated this hypothesis. $CHBr_3$ was mainly detected at $CH^{79}Br^{81}Br^+$ (m/z 172.843), arising from the loss of a Br atom. Accordingly, the signal sensitivity, assessed using the sum of $CH^{79}Br^{81}Br^+$ and its neighboring isotopic peaks (170.844 and 174.840, corresponding to $CH^{79}Br_2^+$ and $CH^{81}Br_2^+$, respectively) was 28.5 ± 0.5 ncps $ppbv^{-1}$ (normalized to 106 cps of $O_2^+$). The correlation coefficient obtained was $R^2$ = 0.997. The detection limit (LD) and quantification limit (LQ) were equal to 13 and 38 pptv, respectively.

Because the instrumental performance was expected to fluctuate throughout the period of the study (3 years), the relative mass-dependent transmission was repeatedly assessed at the beginning of each campaign using a calibration gas standard consisting of a mixture of 14 aromatic compounds (TO-14A Aromatic Mix, Restek Corporation, Bellefonte, USA) (100 ± 10 ppb in nitrogen) that generated protonated nonisotopic molecular ions with mass-to-charge ratio ranging from 79 to 181.

Canisters were connected to the PTR-ToF-MS inlet to quantify $CHBr_3$. The valve of the canister was opened to enable direct PTR-ToF-MS

sampling only when the pressure in the PTR-ToF-MS reaction chamber decreased, indicating that the connection line had been flushed. To provide time for equilibration, the sampling gas passed through the connecting lines for a few measurement cycles.
To ensure consistency between the offline canister and online PTR-ToF-MS measurements, two canisters were sampled near 12X2. The difference between the offline and online measurements was evaluated at a maximum of 30% (Figure S1).

**Water analysis**

*GC-ECD analysis*

Liquid-liquid Extraction (LLE) with 5 mL methyl-tert-butyl ether (MTBE, Chromosolv, HPLC grade, Sigma-Aldrich, Germany) was used for $CHBr_3$ extraction from 50 mL seawater samples. Ten grams of anhydrous $Na_2SO_4$ was added to enhance the extraction efficiency. One milliliter of supernatant was then analyzed on a DB5-ms capillary column (30 m × 0.25 mm × 1 μm). Helium 5.0 was used as a carrier gas at a programmed flow of 1 mL $min^{-1}$, and nitrogen was used as the make-up gas at a flow of 30 mL $min^{-1}$. Calibration curves and analytical performance were determined by the use of a $CHBr_3$ analytical standard purchased from Supelco (Bellefonte, PA, USA) and 1,2-dibromopropane as an internal standard (IS). The injection volume was 1 μL, and the injector temperature was 200 °C. The detector temperature was adjusted to 310 °C. The gas chromatography (GC) oven temperature started at 35 °C, held for 22 min, increased to 145 °C at 20 °C $min^{-1}$, held for 2 min, increased to 225 °C at 20 °C $min^{-1}$, held for 15 min, increased to 280 °C at 10 °C $min^{-1}$, and finally held for 2 min.

*Global parameter analysis*

Anion levels ($Br^-$, $Cl^-$, $SO_4^{2-}$, $NO_3^-$) in water were measured by an ICS-3000 Dionex ion chromatography system using a 30 mM NaOH eluent with a flow rate of 1.5 mL $min^{-1}$ at 30 °C. NPOC and TN were measured using a high-temperature catalytic oxidation technique (Multi N/C 2100, Analytik Jena, Germany). Pretreated samples were injected (50 μL) into a furnace filled with a Pt-preconditioned catalyst. Combustion was realized at 800 °C, and the combustion products were carried by high-purity oxygen (Linde Gas); $CO_2$ was detected by nondispersive infrared (NDIR) spectroscopy, and NO was detected by chemiluminescence (CLD). The LQs were 0.66 mg $L^{-1}$ and 0.34 μg $L^{-1}$ for NPOC and TN, respectively.
$NH_4^+$ analysis was carried out by microplate assays following a protocol described in a previous paper based on $NH_4^+$ derivatization with *o*-phthaldialdehyde (OPA)/N-acetylcysteine (NAC).[43] The method LQ was17.07 μg $L^{-1}$.

### *Modeling of $CHBr_3$ transfer into the air*

The transfer of $CHBr_3$ from water to air was modeled in two areas located in Dock 1 (Figures S2 and S3) using Modelling of Anthropogenic Substances in Aquatic Systems (MASAS).[44] This MS Excel-based tool contains several worksheets; we used the "Processes" and "Two-box model" worksheets, to take into account the strong vertical stratification in the dock area. The measured depth profiles of temperature and salinity were transformed to a density depth profile (Figures S4 and S5) using the international one- atmosphere equation of state of seawater.[45] According to this density stratification, the volumes of an upper and lower box of water were defined. The water exchange between these two boxes by turbulent diffusivity was calculated using the stability frequency (Brunt-Väisälä- frequency) via equation 22-31 from Schwarzenbach et al. (2003), given as equation S3 in the Supporting Information (SI-1, pages S10-S12).[46] The model considered that both boxes were subject to water flushing and the upper box was subject to gas exchange with the atmosphere. Flushing was modeled using the water flow measured by the flow meter integrated across the depth of the box, the cross-sectional area of the box and its volume. Gas exchange was modeled with the two-surface-film model integrated in MASAS using the following parameters: mean depth of the upper box, average wind speed at 10 m above ground on the day of water sampling, Henry coefficient for $CHBr_3$ calculated for the water temperature of the upper box as outlined in Quack and Wallace (2003),[1] aqueous diffusion coefficient of $5.69 \times 10^{-6}$ $cm^2$ $s^{-1}$, gas-phase diffusion coefficient of 0.064 $cm^2$ $s^{-1}$, and exponents a and b set to 0.7 for turbulent waters. No other removal processes for $CHBr_3$ were considered in the model. The worksheet "Processes" was used to calculate the total elimination rate constant for $CHBr_3$ for each box, and the obtained values were thereafter used in the worksheet "Two-box-model". Furthermore, the percent contribution of gas exchange to the total removal was obtained. Using the worksheet "Two-box-model" allowed us to quantify the production rate of $CHBr_3$ in each box to obtain the measured aqueous concentration in each box. The total production rate, percentage of gas exchange, and area of the model were finally used to calculate, the sea-to-air flux in mg $m^{-2}$ $day^{-1}$, as explained in equation S6 in the Supporting Information (SI-1).

## Results and discussion

### *General weather conditions*

During the first campaign carried out in spring (Apr. 2017), samples were collected in a sustained southeasterly wind (35-40 km $h^{-1}$ on average) with gusts. Both summer (June 2018 and June 2019) and fall (Oct. 2017 and Nov. 2018) campaigns were carried out under similar wind conditions, i.e., sustained and then moderate mistral. The winter (Feb. 2018) campaign took place with a relatively weak north wind, which then shifted to the northwest.

The average air temperature during the sampling campaigns was 6 °C in winter, from 15 to 24 °C in summer, and from 15 to 17 °C in fall. Only

minor precipitation occurred during the campaign of fall 2018 (approximatively 4.5 mm).
Seawater temperature influences the chlorination rate (see section 2.1), formation kinetics of $CHBr_3$ in water, and air-water exchange of $CHBr_3$ (due to turbulence induced by the wind conditions and salinity gradient), as the Henry's Law constant values show that when the temperature rises, $CHBr_3$ is less soluble in seawater.[47] In Feb. 2018, the seawater temperatures were between 11 and 12 °C, indicating no or very low use of electrochlorination. Except for that campaign, the seawater temperatures ranged between 15 and 21 °C. At the industrial outlets, the cooling water effluents were between 2 and 5 °C warmer than the pumped water, whereas the heating water effluents (LNG terminals) were between 2 and 6 °C cooler than the pumped water (Table S2).

***Bromoform levels in seawater***

$CHBr_3$ was found in industrial discharges during each sampling campaign (Figure 2, top, and Table S2), with higher levels found in summer (mean: 6.6 µg $L^{-1}$; median: 6.20 µg $L^{-1}$; min.: 0.1 µg $L^{-1}$; max.: 34.6 µg $L^{-1}$; n = 20), in fall (mean: 3.1 µg $L^{-1}$; median: 2.7 µg $L^{-1}$; min.: 0.05 µg $L^{-1}$; max.: 10.0 µg $L^{-1}$; n = 25) and in spring (mean: 4.0 µg $L^{-1}$; median: 1.7 µg $L^{-1}$; min.: 0.2 µg $L^{-1}$; max.: 11.4 µg $L^{-1}$; n = 12) than in winter (mean: 1.4 µg $L^{-1}$; median: 0.1 µg $L^{-1}$; min.: 0.1 µg $L^{-1}$; max.: 3.7 µg $L^{-1}$). The highest levels were generally found in cold water discharges (8X1, 8X2, 12X1, 12X2, and 12X), with amounts between 0.5 and 11.4 µg $L^{-1}$ (mean: 7.8 µg $L^{-1}$; median: 8.0 µg $L^{-1}$; n = 22) ranging up to 34.6 µg $L^{-1}$ (8X2, June 2019). $CHBr_3$ in hot water discharges was generally lower (mean: 2.2 µg $L^{-1}$; median: 1.1 µg $L^{-1}$; n = 55) with some exceptions observed in outlets 9X and 10X during half of the campaigns (up to 10.2 µg $L^{-1}$).
The pH measured in all water samples during the different campaigns was always above 8.1, indicating that the bromine species resulting from the rapid reaction between electrogenerated $HOCl/OCl^-$ and natural $Br^-$ were mainly HOBr and $OBr^-$ (the concentrations of other species such as BrCl, BrOCl, $Br_2O$, and $Br_2$ are five to eight orders of magnitude smaller, as previously shown by Heeb et al.).[23] Once formed in water, HOBr and $OBr^-$ are very reactive toward phenolic groups (leading to the formation of high- and low-molecular- weight brominated organic byproducts, including $CHBr_3$)[18], ammonia and amines (leading to the formation of bromamines), sulfamides and S-containing compounds.[48] Rate constants for the reaction of $HOBr/OBr^-$ are, however, slightly higher for ammonia and amines ($k = 4\text{-}7.5 \times 10^7$ $M^{-1}$ $s^{-1}$)[23] than for aromatic organic compounds (for example, $6.5 \times 10^5$ $M^{-1}$ $s^{-1}$ for phenol at pH = 7).[49] Therefore, the levels of $NH_4^+$ in discharged waters were systematically lower than those found in pumped waters (Table S2: 8X1 and 8X2 are pumped from 2C ; 9X from 4P ; and 10X, 11X, and 12X from 6P) and were assumed to react with $HOBr/OBr^-$ to be transformed into bromamines. A slight pattern seems to indicate that the level of $CHBr_3$ in water was reduced when higher levels of $NH_4^+$ were present in the pumped waters (Figure S6), following the apparent rate constants given above. However, this trend was only valid for

some specific industrial outlets (9X and 10X), which seems to demonstrate that other factors (including the presence of other amine compounds or DOM moieties within the pipes) should be considered to explain the variation in $CHBr_3$ found in waters.

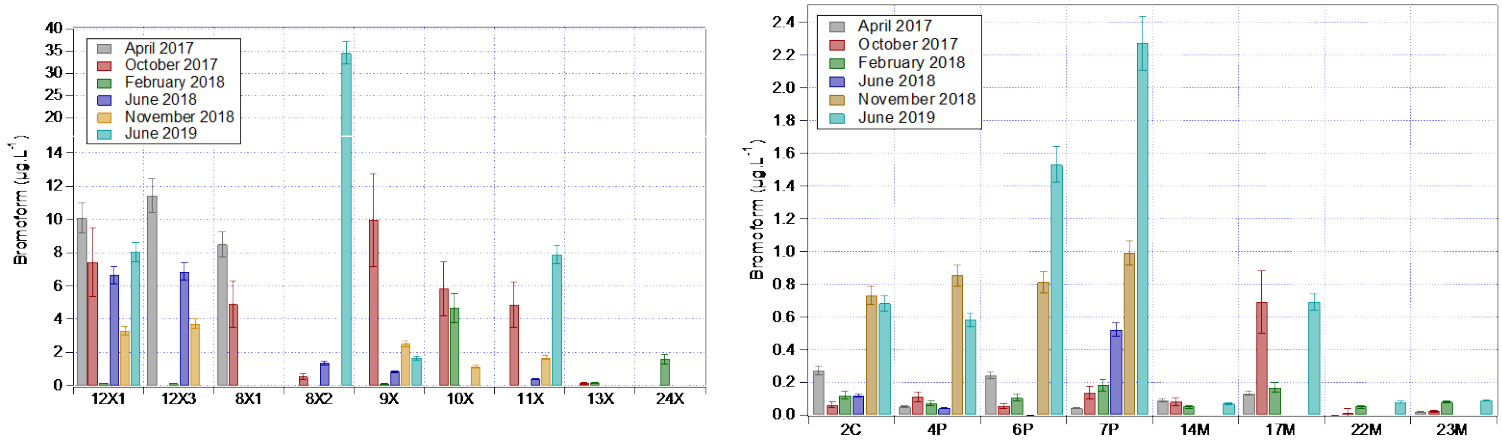


*Figure 2: $CHBr_3$ levels found during the different campaigns in industrial outlets (top) and in offshore sampling points (bottom)*

The levels of $CHBr_3$ found at sampling sites other than industrial outlets (Figure 2, bottom) were ten to thirty times lower, with values between 0.047 µg $L^{-1}$ (LQ) and 2.3 µg $L^{-1}$ (7P, June 2019). These low levels nevertheless exceed by 100-10,000 times the reported levels linked to the natural production of $CHBr_3$ (between 0.03 and 0.15 ng $L^{-1}$ in the open ocean),[31] and the levels of natural $CHBr_3$ reported near coastal areas not impacted by chlorinated discharges (between 4.3 and 10.6 ng $L^{-1}$).[31] Table S3 provides an overview of reported marine surface concentrations of $CHBr_3$; the concentrations show large variations with respect to geographic location (higher in equatorial regions, in upwelling areas, near coastal areas and in shelf regions).[31,50-52] The $CHBr_3$ levels found at sampling sites located far from the industrial discharge points (such as values up to 0.7 µg $L^{-1}$ for 17M and up to 0.08 µg $L^{-1}$ for 22M) are thus assumed to derive from $CHBr_3$ that was anthropogenically formed during the electrochlorination of seawater. The difference between the levels found in outlets and offshore areas is thus assumed to be linked to either the high

dilution coefficient in the Gulf of Fos and/or volatilization.

**Bromoform in the air**

*Off-line measurements*

$CHBr_3$ was detected in all samples collected in the air by canisters (Figure 3). The atmospheric mixing ratios of $CHBr_3$ measured during the six field campaigns showed values spanning three orders of magnitude from 9 ± 4 pptv (6P, Feb. 2018) to 3.9 ± 0.2 ppbv (12X1, Nov. 2018).

The highest levels were clearly found in the vicinity of industrial discharges (Figure 3, top), with the highest level at 12X1, corresponding to the ORV (heat exchanger).

Mixing ratios between 820 ± 58 pptv (June 2019) and 3.9 ± 0.2 ppbv (Nov. 2018) were observed as a function of chlorination level. In June 2019, some chlorination units were out of service, leading to 50% less chlorination than normal. This explains why the $CHBr_3$ level was 3 to 5 times lower than those for the other campaigns (Apr. 2017, Oct. 2017, June 2018, and Nov. 2018) when the chlorination was operating at full capacity. In contrast, in Feb. 2018, in the absence of electrochlorination (colder seawater temperature), the $CHBr_3$ mixing ratio remained considerably lower, i.e., 46 ± 11 pptv.

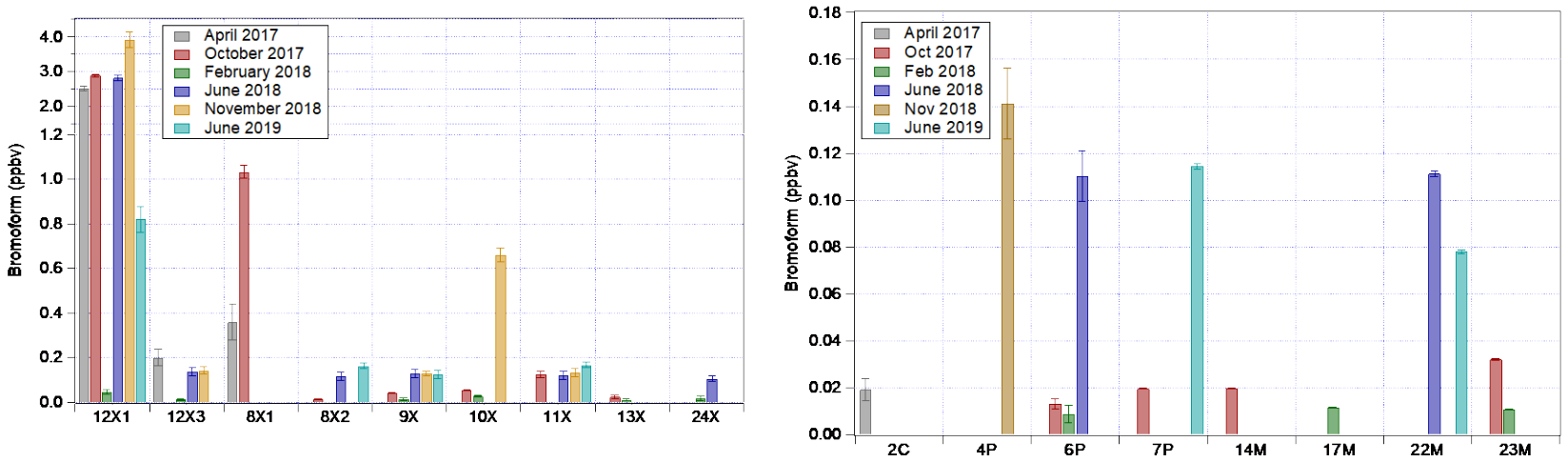


*Figure 3. $CHBr_3$ mixing ratios (ppbv) measured during 6 field campaigns on 17 sampling sites (on the top: levels in industrial outlets; on the bottom: levels in offshore sampling points).*

To a lesser extent, $CHBr_3$ levels were also high at the outlets of the various industrial facilities in the Gulf, i.e., the LNG terminals (8X and 12X), power plants (9X, 10X, and 24X), and steel industry facility (11X). When these industries use chlorination, they discharge large volumes of warmer water than the surrounding waters into the Gulf. Therefore, the water density decreases at the sea surface which promotes ocean-atmosphere exchange of volatile $CHBr_3$.[34] Indeed, the average $CHBr_3$ mixing ratio was 214 pptv (median: 132 pptv; min.: 12 pptv; max.: 350 pptv).These measurements at the outlets (Figure 3: 8X, 9X, 10X, 11X, 13X, and 24X in Apr. 2017, Oct. 2017, June 2018, Nov. 2018, and June 2019) should be compared with those on Feb. 2018 when there was no chlorination. The average $CHBr_3$ mixing ratio would then be 16 pptv (median: 14 pptv; min.: 11 pptv; max.: 28 pptv).

For the offshore sampling points (Figure 3: 7P, 14M, 17M, 22M, and 23M, including the harbor basins (4P and 6P) in Oct. 2017, June 2018, Nov. 2018, and June 2019), the average CHBr3 mixing ratio was 64 pptv (median: 78 pptv; min.: 13

pptv; max.: 141 pptv). Even if these sampling points were far from industrial cooling water discharge areas, a decrease in $CHBr_3$ levels was observed when there was no electrochlorination; i.e., the average $CHBr_3$ mixing ratio was 18 pptv (median: 12 pptv; min.: 9 pptv; max.: 32 pptv).

Figure 4 summarizes the average levels of $CHBr_3$ in the different measurement areas, i.e., ORV (12X1), outlets (8X, 9X, 10X, 11X, 13X, and 24X), and harbor basins and sea (4P, 6P, 7P, 14M, 17M, 22M, and 23M) in the Gulf of Fos. Electrochlorination was considered at full capacity during Apr. 2017, Oct. 2017, June 2018, and Nov. 2018. There was no electrochlorination during the sampling campaign of Feb. 2018.
Sampling sites 12X1, 12X2, and 12X correspond to the ORV (starting point of electrochlorination), the midpoint of a 650 m-long canal allowing draining of electrochlorinated water to the sea, and the discharge point, respectively. A $CHBr_3$ concentration decrease of approximatively 90% was systematically observed along these three points, suggesting a rapid dilution to air (from 2.5 ± 0.1 ppbv (12X1) to 200 ± 37 pptv (12X) on Apr. 2017, from 2.8 ± 0.1 ppbv (12X1) to 137 ± 20 pptv (12X) in June 2018, and from 3.9 ± 0.2 ppbv (12X1) to 142 ± 16 pptv (12X) in Nov. 2018). This trend in the air was also observed in the water (the $CHBr_3$ level decreased by approximatively 75% between 12X1 and 12X).
When the electrochlorination process was inactive, the bromoform levels were consistent between sampling points and were of the same order of magnitude as the natural atmospheric bromoform mixing ratios observed in coastal areas.[30]

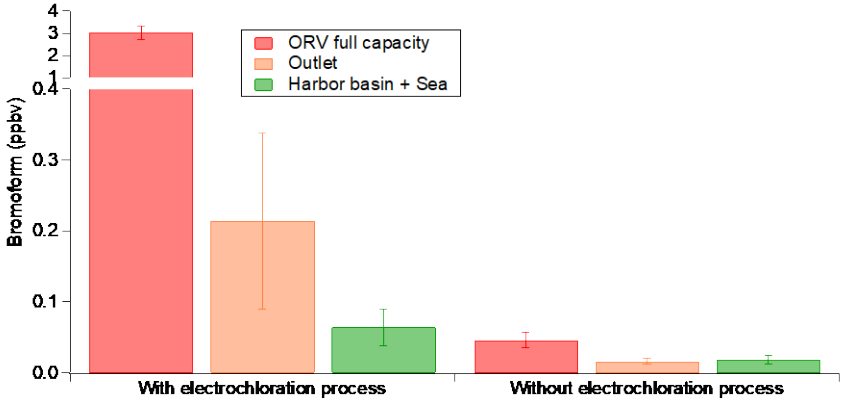


*Figure 4. Average $CHBr_3$ mixing ratios (ppbv) in different typologies of sites, with or without electrochlorination*

*On-line measurements*

During four field campaigns (Oct. 2017, Feb. 2018, June 2018, and June 2019), $CHBr_3$ was monitored online with high time resolution at one of the LNG terminals (12X2) (Figure 5).

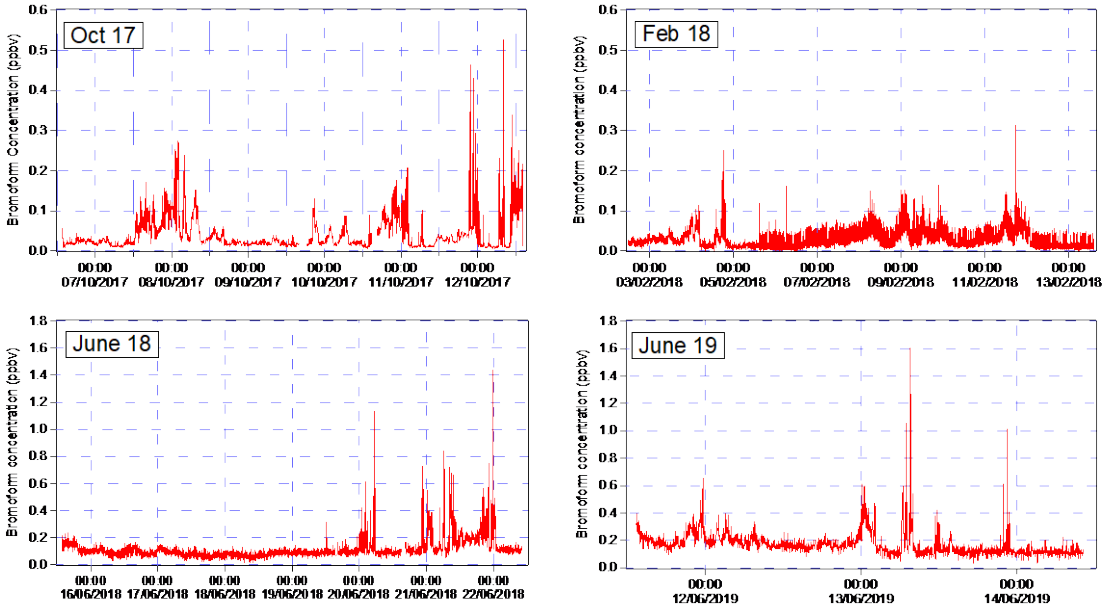


Figure 5. Online monitoring of $CHBr_3$ mixing ratio (ppbv) at the 12X2 sampling point

These measurements revealed rapid (a few minutes) and significant (up to two orders of magnitude) variations in $CHBr_3$ levels, i.e., from <LD to 527 pptv on Oct. 2017, from <LD to 313 pptv in Feb. 2018, from 14 pptv to 1.4 ppbv in June 2018, and from 34 pptv to 1.6 ppbv in June 2019.
At the outlet, the cooling water discharge rate was regulated by the LNG terminal and was not constant over time. However, these changes in flow rate were slow and could not explain the rapid variations in atmospheric $CHBr_3$ levels observed. There was also no correlation between the mixing ratios of $CHBr_3$ and i) those of VOCs that can characterize industrial activity (e.g., butene, benzene, toluene, xylenes, naphthalene), ii) the presence of a gas tanker tied up at the LNG terminal, or iii) the activity of the LNG storage tanks.
It can therefore be assumed that the rapid variations in $CHBr_3$ levels were due to sudden changes in wind direction, which suggests potential high $CHBr_3$ concentration levels near the sampling site.

*Pollution roses*
The geographical origin of the measured $CHBr_3$ was determined using ZeFir (v.3.60).[53] Figure S7 is based on nonparamagnetic regressions from input data, i.e., measured $CHBr_3$ concentrations and wind data (speed and direction). The wind data come from the station of Météo-France Port-de-Bouc, which is representative of the overall meteorological conditions at this sampling point. However, as reported before, topography can occasionally lead to specific air flows and can induce a specific and local distribution of wind speed and direction.
According to the continuous monitoring of gaseous $CHBr_3$, pollution roses make it possible to model and therefore visualize the average $CHBr_3$ level observed at a sampling site as a function of the wind regime. The higher the $CHBr_3$ level is, the more the sampling site is influenced by the emission sources for the wind sector considered.
Figure S7 illustrates the pollution rose for the 12X2 sampling site for the field campaigns with continuous measurement, i.e., Oct. 2017, Feb. 2018, June 2018, and June 2019. All campaigns were carried out under mistral (northwest wind), which was sustained and then moderate in summer and fall (>15- 20 km $h^{-1}$) and, relatively weak in winter (5-15 km $h^{-1}$).
The modeled $CHBr_3$ levels for Feb. 2018, were low. Industrial facilities used little or no chlorination because of the low seawater temperature. Moreover, there was no contribution of $CHBr_3$ in the northwest wind direction, suggesting that there was no long-distance transport of $CHBr_3$.
During the fall and summer field campaigns, $CHBr_3$ levels did not follow the mistral wind regime. When the wind speed was low, the presence of $CHBr_3$ was independent of the wind direction and when the wind speed increased, $CHBr_3$ generally came from the Gulf. These observations highlight that the measured $CHBr_3$ came from local sources.
The pollution roses also model $CHBr_3$ levels ranging from approximatively 150 pptv to 300 pptv in summer and from approximatively 60 pptv to

120 pptv in fall. These modeled values highlight the large contribution of industrial activities, i.e., the electrochlorination of seawater, to the formation of atmospheric $CHBr_3$.

**Modeling of the sea-to-air emission of $CHBr_3$**

The daily flux of $CHBr_3$ from water to air was modeled for Dock #1 which hosts four industrial plants that discharge chlorinated waters (Figure 1), either cold discharges (8X), or hot discharges (9X, 10X, and 11X), and which receive a large inflow of freshwater from the Rhône River. Table 1 shows the model input parameters and the model results for four campaigns. The northern part of Dock #1 was stratified with less dense channel water overlying seawater, while this stratification was not present in the southern part on one occasion. The modeled $CHBr_3$ sea-to-air fluxes ranged from 0.02 to 16.1 mg $m^{-2}$ $day^{-1}$. The lowest flux was found in the northern dock in Feb. 2018 when no electrochlorination was active. In Oct. 2017, when chlorination was active at the northern dock the flux was 0.45 mg $m^{-2}$ $day^{-1}$.[1] All other fluxes were higher than this value. The highest flux was calculated for the northern dock area when $CHBr_3$ was highest in water, together with a very favorable density stratification for $CHBr_3$ transfer to the atmosphere, with only 0.66 m of water in an upper box layer exposed to wind overlaying denser water. In the southern part of the dock, where three chlorination plants were active, the fluxes were not higher than the highest flux in the north because the generally thicker upper box layer caused lower removal rates of $CHBr_3$ to the atmosphere under the same wind conditions

The incorporation of measured water flows into the model showed that the water was renewed in the dock area at high rates, and thus that significant amounts of $CHBr_3$ were also transported to the Gulf.

The modeled fluxes were compared with the measured atmospheric mixing ratios in canisters taken on the docks (Figure S8). The comparison shows that lower atmospheric mixing ratios were consistent with lower modeled sea-air fluxes, and vice versa.

**Environmental and health implications**

$CHBr_3$ is one of the major byproducts generated during (electro)chlorination of seawater and released into the sea.[16-18,52,54-56] The levels found in water, -including the present results-, are far below the toxicity levels reported in the literature for marine organisms (2.9 mg $L^{-1}$ for *C. variegatus* (fish) with 96 h-mortality as the endpoint;[57] 184.5 mg $L^{-1}$ for *P. dumerilii* (polychaete) with $EC_{50}$ Embryo Developmental Toxicity as endpoint;[58] 133 mg $L^{-1}$ for *P. lividus* embryos (ursin) with EC50 embryo developmental toxicity as endpoint).[28]

From a human health point of view, $CHBr_3$ is not classifiable regarding its carcinogenicity to humans (Group 3) by the International Agency for Research on Cancer,[58]while the US Environmental Protection Agency (US EPA) has concluded that $CHBr_3$ is a probable human carcinogen (Group

B2).[59] Acute and chronic exposure to humans from inhalation of $CHBr_3$ has not yet been studied. However, based on animal model on studies, the US EPA has estimated the probability of an individual developing cancer from breathing air containing bromoform. The US EPA calculated an inhalation unit risk of 1.1 × 10-6 $m^3$ $\mu g^{-1}$ ; i.e.,if a person were to continuously breathe air containing $CHBr_3$ at an average concentration of 87 pptv (0.9 $\mu g\ m^{-3}$) over her or his entire lifetime, theoretically, that person would have no more than a one-in-a-million increased chance of developing cancer.[59] According to this threshold value of inhalation exposure, the measured (Figure 2) and modeled (Figure 4) mixing ratios of $CHBr_3$ highlight that the contribution of industrial activities, i.e., the electrochlorination of seawater, could have limited health adverse effects on the staff working at these industrial sites and the general population living nearby.

The levels of $CHBr_3$ found in the atmosphere are a cause for major concern, as the levels measured during the present study greatly exceed (by up to 100 times) the reported or modeled values of natural release into the atmosphere, and the reported atmospheric concentrations measured at a local or regional scale.[1,2,34-36,50-52] However, our results should be considered from several perspectives. On the one hand, our results were obtained in a very localized area (42 $km^2$), whereas published modeled data are based on a considerably larger area (sometimes at a subcontinent scale); therefore, the contribution of anthropogenic $CHBr_3$ issued from the industrialized area of the Gulf of Fos to global $CHBr_3$ emissions could be neglected. On the other hand, several other anthropogenic sources are located on the French Mediterranean coasts and around the Mediterranean Sea. For example, many wastewater plants disinfect waters with chlorine (at $Cl_2$ doses between 2.4 and 2.7 mg $L^{-1}$), as required by several European directives *to provide protection to humans against exposure to waterborne pathogenic microorganisms*, and to *prevent the spread of human pathogenic microorganisms from wastewater effluents to aquatic environments especially from fecal contamination*.[62] The exact volume of disinfected waters released into the sea remains unknown, and consequently, the amount of $CHBr_3$ issued from these treatments also remains unknown. The only data available to date are the number of European wastewater treatment plants that use disinfection before release (see map SI-2 in the Supporting Information).

Another source of anthropogenic $CHBr_3$ comes from discharges of ballast water. In general, vessels discharge ballast water when loading cargo, and take up ballast water when unloading cargo. Therefore, the majority of ballast water operations are carried out in or close to ports. This water has to be disinfected before release; disinfection with chlorine (or electrochlorination) is the most commonly used process.[57] The annual global ballast water discharge from vessels engaged in international seaborne trade was estimated to be 3.1 billion tons in 2013.[63] $CHBr_3$ is the most encountered disinfection byproduct (DBP) in ballast water, with levels reaching 890 $\mu g\ L^{-1}$.[25] The amount of $CHBr_3$ in the Gulf of Fos, or even at the Mediterranean Sea- levels, issuing from ballast waters remain also unknown.

Other identified sources of anthropogenic $CHBr_3$ come from desalination plants. To date, approximatively 30 million cubic meters is produced per

day in the countries of the Mediterranean Rim (44% of which is produced in Spain), and the seawater consumption of desalination plants is equivalent to 3 to 8 times the amount of freshwater produced (depending on whether thermal or reverse osmosis treatment is applied). Brine and reverse osmosis discharges into the sea cause significant levels of $CHBr_3$, either in water or directly in air (up to 90% of $CHBr_3$ is discharged as vent gases).[19,64]

$CHBr_3$ has an atmospheric lifetime of 2-3 weeks,[61] and according to season and location of emissions, it may deplete the ozone layer by catalytic cycles (after stratospheric uplifts, mainly in regions of high-reaching convective activity such as the tropical Indian Ocean and subtropical northern Atlantic) or may i) have an impact on the oxidizing capacity of the atmosphere by changing OH concentrations and perturbing the OH-to-$HO_2$ ratio toward OH, leading to an increase in $CH_4$ in the troposphere,[33,62] ii) influence new particle formation and iii) control the formation of cloud condensation nuclei.[4,12]

Improving atmospheric chemistry models requires better knowledge of the concentration levels of $CHBr_3$ at potentially high emission sources, such as along the coast of the Mediterranean Sea where data are very scarce or even completely non-existent. Inventorying and quantifying these different anthropogenic sources of $CHBr_3$ will allow us to better characterize and understand the oxidizing capacity of the atmosphere.

**Acknowledgements**

This work was supported by the Doctoral School of "Environmental Sciences" (ED251) at Aix- the French National Research Agency (ANR) within the project FOSSEA (ANR-16-CE340009). The authors also acknowledge ELENGY for providing access to its industrial plant and allowing the mobile laboratory (12X) to be installed as closely as possible to the discharge sites.

**Competing financial interests**

The authors declare no competing financial interests.

**Supporting Information**

The supporting information includes a detailed description of study site and sampling periods; all physical-chemical parameters characterizing the inlets, outlets and sea samples; the gas-phase $CHBr_3$ measurements obtained by PTR-ToF-MS after sampling by either canister or laboratory truck; the correlation between $CHBr_3$ detected in water and NPOC/$NH_4^+$ ratio; histograms showing the levels of $CHBr_3$ in air with and without electrochlorination; the pollution roses at 12X2 showing that the measured $CHBr_3$ is readily formed by industrial plants; the correlation curve between model sea-to-air $CHBr_3$ and observed levels; and details about the modeling of sea-air fluxes.

Table 1. Model input parameters and model results

| Model Input Parameters | Unit | Northern Dock 8X | | | | Southern Dock 10X | | | |
|---|---|---|---|---|---|---|---|---|---|
| | | October 2017 | February 18 | June 2018 | June 2019 | October 2017 | February 2018 | June 2018 | June 2019 |
| $CHBr_3$ at the surface | mg $m^{-3}$ | 1.4 | 0.218 | 1.37 | 34.6 | 5.84 | 4.68 | 4.51 | 10.22 |
| $CHBr_3$ Conc at depth | mg $m^{-3}$ | 0.04 | 0.11 | 4.6 | 4.95 | 0.94 | 9.63 | 0.11 | 0 |
| Stratification at …. | m | 1 | 1 | 1.4 | 0.66 | 1.7 | No stratification | 2 | 3.5 |
| Water exchange between layers | $m^3$ $day^{-1}$ | 10534 | 6307 | 7660 | 2900 | 97516 | Not applicable | 48123 | 352600 |
| Water flow velocity in inflow | m $s^{-1}$ | 0.39 | 0.61 | 0.04 | 0.13 | 0.3 | 0.7 | 0.1 | 0.05 |
| Wind speed at 10 m above ground | m $s^{-1}$ | 4 | 2 | 3 | 4 | 4 | 2 | 3 | 4 |
| Model results | | | | | | | | | |
| Water removal rate in upper layer | $day^{-1}$ | 1.4 | 2.2 | 0.2 | 0.31 | 1.75 | 12.27 | 0.69 | 0.6 |
| TBM removal rate to atmosphere | $day^{-1}$ | 0.3 | 0.164 | 0.158 | 0.454 | 0.179 | 0.032 | 0.112 | 0.087 |
| TBM removal rate in upper layer | $day^{-1}$ | 1.7 | 2.36 | 0.36 | 0.76 | 1.93 | 12.3 | 0.8 | 0.69 |
| Needed daily input of TBM | kg $day^{-1}$ | 1.5 | 0.2 | 3.5 | 16 | 28 | 500 | 10.5 | 38 |
| Daily loss of $CHBr_3$ to air | kg $day^{-1}$ | 0.26 | 0.01 | 1.54 | 9.52 | 2.6 | 1.3 | 1.47 | 4.8 |
| $CHBr_3$ flux from sea to air | mg $m^{-2}$ $day^{-1}$ | 0.45 | 0.02 | 2.59 | 16.06 | 4.38 | 2.19 | 2.48 | 8.1 |

## References

(1) Quack, B.; Wallace, D.W.R. Air-sea flux of bromoform: Controls, rates, and implications. *Glob. Biogeochem. Cycles* **2003**, *17*, GB1023.
(2) Chipperfield, M.P.; Hossaini, R.; Montzka, S.A.; Reimann, S.; Sherry, D.; Tegtmeier, S. Renewed and emerging concerns over the production and emission of ozone-depleting substances. *Nat. Rev. Earth Environ.* **2020**, 1, 251-263.
(3) Mithoo-Singh, P.K.; Keng, F.S.L.; Phang, S.M.; Leedham Elvidge, E.C.; Sturges, W.T.; Malin, G.; Abd Rahman, N. Halocarbon emissions by selected tropical seaweeds: species-specific and compound-specific responses under changing pH. *PeerJ*. **2017,** 5, e2918.
(4) Hughes, C.; Sun, S. Light and brominating activity in two species of marine diatom. *Mar. Chem*. **2016**, 181, 1-9.
(5) Yang, B., Yang, G.-P., Lu, X.-L., Li, L., He, Z. Distributions and sources of volatile chlorocarbons and bromocarbons in the Yellow Sea and East China Sea. *Mar. Pollut. Bull*. **2015**, 95, 491-502.
(6) Weinberg, I.; Bahlmann, E.; Eckhardt, T.; Michaelis, W.; Seifert, R.A. Halocarbon survey from a seagrass dominated subtropical lagoon, Ria Formosa (Portugal): flux pattern and isotopic composition. *Biogeosciences* **2015**, 12, 1697-1711.
(7) Hughes, C.; Johnson, M.; Utting, R.; Turner, S.; Malin, G.; Clarke, A.; Liss, P.S. Microbial control of bromocarbon concentrations in coastal waters of the western Antarctic Peninsula. *Mar. Chem*. **2013**, 151, 35-46.
(8) Malin, G.; Wilson, W.H.; Bratbak, G.; Liss, P.S.; Mann, N.H. Elevated production of dimethylsulfide resulting from viral infection of cultures of Phaeocystis pouchetii. *Limnol. Oceanogr*. **1998**, 43, 1389-1393.
(9) Herwig, R.; Cordell, J.; Perrins, J.; Dinnel, P.; Gensemer, R.; Stubblefield, W.; Ruiz, G.; Kopp, J.; House, M.; Cooper, W. Ozone treatment of ballast water on the oil tanker S/TTonsina: chemistry, biology and toxicity. *Mar. Ecol. Prog. Ser.* **2006**, 324, 37-55.
(10) Wever, R.; van der Horst, M.A. The role of vanadium haloperoxidases in the formation of volatile brominated compounds and their impact on the environment. *Dalton Trans.* **2013**, 42, 11778-11786.
(11) Liu, Y.; Thornton, D.C.O.; Bianchi, T.S.; Arnold, W.A.; Shields, M.R.; Chen, J.; Yvon-Lewis S.A. Dissolved Organic Matter Composition Drives the Marine Production of Brominated Very Short-Lived Substances. *Environ. Sci. Technol*. **2015**, 49, 3366−3374.
(12) He, Z.; Yang, G.P.; Lu, X.L.; Zhang H.H. Distributions and sea-to-air fluxes of chloroform, trichloroethylene, tetrachloroethylene, chlorodibromomethane and bromoform in the Yellow Sea and the East China Sea during spring. *Environ. Pollut*. **2013**, 177, 28-37.
(13) Hepach, H.; Quack, B.; Tegtmeier, S.; Engel, A.; Bracher, A.; Fuhlbrügge, S.; Galgani, L.; Atlas, E.L.; Lampe, J.; Frieß, U.; Krüger, K. Biogenic halocarbons from the Peruvian upwelling region as tropospheric halogen source. *Atmos. Chem. Phys*. **2015**, 15, 13647-13663.
(14) Fiehn, A.; Quack, B.; Hepach, H.; Fuhlbrügge, S.; Tegtmeier, S.; Toohey, M.; Atlas, E.; Krüger, K. Delivery of halogenated very short-lived substances from the west Indian Ocean to the stratosphere during the Asian summer monsoon. *Atmos. Chem. Phys.* **2017**, 17, 6723–6741.
(15) Fuhlbrügge, S.; Quack, B.; Tegtmeier, S.; Atlas, E.; Hepach, H.; Shi, Q.; Raimund, S.; Krüger, K. The contribution of oceanic halocarbons to marine and free troposphere air over the

tropical West Pacific. *Atmos. Chem. Phys.* **2016***,* 16, 7569–7585.
(16) Khalanski, M. & Jenner, H. A. (2012). Chapter 9: Chlorination chemistry and ecotoxicology of the marine cooling water systems, 183-226. In Rajagopal, S.; Jenner, H. A. & Venugopalan, V. P. (Eds) Operational and environmental consequences of large industrial cooling water systems, Springer Science Publisher, 491 pp..
(17) Boudjellaba, D.; Dron, J.; Revenko, G.; Demelas, C.; Boudenne, J.-L. Chlorination by-product concentration levels in seawater and fish of an industrialized bay (Gulf of Fos, France) exposed to multiple chlorinated effluents. *Sci. Total Environ.* **2016**, 541, 391-399.
(18) Manasfi, T.; Lebaron K; Verlande M.; Dron J.; Demelas C.; Vassalo L.; Revenko G.; Boudenne J.L. Occurrence and speciation of chlorination byproducts in marine waters and sediments in a semi-enclosed bay exposed to industrial chlorinated effluents. *Int. J. Hyg. Environ. Health*. **2019**, 222(1), 1-8.
(19) Le Roux, J.; Nada, N.; Khan M.T.; Croué, J.P. Tracing disinfection byproducts in full-scale desalination plants. *Desalination*. **2015**, 359, 141-148.
(20) Agus, E.; Sedlak, D.L. Formation and fate of chlorination by-products in reverse osmosis desalination systems. *Water Res*. **2010**, 44 (5), 1616-1626.
(21) IMO, 2008. Guidelines for Approval of Ballast Water Management Systems (G8). Resolution MEPC.174(58). International Maritime Organization, London.
(22) Ding, G.; Zhang, X.; Yang, M.; Pan, Y. Formation of new brominated disinfection byproducts during chlorination of saline sewage effluents. *Water Res*. **2013**, 2710-2718.
(23) Heeb, M.B., Criquet, J., Zimmermann-Steffens, S.G., von Gunten, U. Oxidative treatment of bromide-containing waters : Formation of bromine and its reactions with inorganic and organic compounds - A critical review. *Water Res*. **2014**, 15-42.
(24) Deborde, M.; von Gunten, U. Reactions of chlorine with inorganic and organic compounds during water treatment—Kinetics and mechanisms: A critical review. *Water Res*. **2008**, 42, 13-51.
(25) Maas, J.; Tegtmeier, S.; Jia, Y.; Quack, B.; Durgadoo, J.V.; Biastoch, A.. Simulations of anthropogenic bromoform indicate high emissions at the coast of East Asia. *Atmos. Chem. Phys*. **2021**, 21, 4103-4121.
(26) Mazik, K.; Hitchman, N.; Quintino, V.; Taylor, C.J.L., Butterfield, J.; Elliott, M. Sublethal effects of a chlorinated and heated effluent on the physiology of the mussel, Mytilus edulis L.: A reduction in fitness for survival? *Mar. Pollut. Bull*. **2013**, 77, 123-131.
(27) Taylor, C.J.L. The effects of biological fouling control at coastal and estuarine power stations. *Mar. Pollut. Bull*. **2006**, 53, 30-48.
(28) Lebaron, K.; Mechiri, L.; Richard, S.; Austruy, A.; Boudenne, J.-L.; Coupé, S. Assessment of individual and mixed toxicity of bromoform, tribromoacetic-acid and 2,4,6 tribromophenol, on the embryo-larval development of *Paracentrotus lividus* sea urchin. *Environ. Sci. Pollut. Res.* **2019**, 26(20), 20573-20580.
(29) Moore, R.M.; Geen, C.E.; Tait, V.K. Determination of Henry law constants for a suite of naturally occurring halogenated methanes in seawater, *Chemosphere*. **1995**, 30, 1183-1191.
(30) Carpenter, L.J.; Liss, P.S. On temperate sources of bromoform and other reactive organic bromine gases. *J. Geophys. Res*. **2000**, 105(D1, 20539-20547,
(31) Ziska, F.; Quack, B.; K. Abrahamsson, K.; Archer, S.D.; Atlas, E.; Bell, T.; Butler, J.H.; Carpenter, L.J.; Jones, C.E.; Harris, N.R.P.; Hepach, H.; Heumann, K.G.; Hughes, C.; Kuss,

J.; Kruger, K.; Liss, P.; Moore, R.M.; Orlikowska, A.; Raimund, S.; Reeves, C.E.; Reifenhauser, W.; Robinson, A.D.; Schall, C.; Tanhua, T.; Tegtmeier, S.; Turner, S.; Wang, L.; Wallace, D.; Williams, J.; H. Yamamoto, H.; Yvon-Lewis, S.; Yokouchi, Y. Global sea-to-air flux climatology for bromoform, dibromomethane and methyl iodide. *Atmos. Chem. Phys.* **2013**, 13, 8915-8934.
(32) Hughes, C.; Chuck, A.L.; Rossetti, H.; Mann, P.J.; Turner, S.M.; Clarke, A.; Chance, R.; Liss, P.S. Seasonal cycle of seawater bromoform and dibromomethaneconcentrations in a coastal bay on the western Antarctic Peninsula. *Glob. Biogeochem. Cycle*. **2009**, 23, GB2024, 1-13.
(33) Hossaini, R.; Chipperfield, M.P.; Monge-Sanz, B.M.; Richards, N.A.D.; Atlas, E.; Blake, D.R. Bromoform and dibromomethane in the tropics: a 3-D model study of chemistry and transport. *Atmos. Chem. Phys*. **2010**, 10, 719-735.
(34) Palmer, C.J.; Reason, C.J. Relationships of surface bromoform concentrations with mixed layer depth and salinity in the tropical oceans. *Glob. Biogeochem. Cycle***. 2009**, 23, GB2014, 1-10.
(35) Maas, J.; Tegtmeier, S.; Quack, B.; Biastoch, A.; Durgadoo, J.V.; Rühs, S.; Gollasch, S.; David M. Simulating the spread of disinfection by-products and anthropogenic bromoform emissions from ballast water discharge in Southeast Asia. *Ocean Sci*. **2019**, 15, 891-904.
(36) Mehlmann, M.; Quack, B.; Atlas, E.; Hepach, H.; Tegtmeier, S. Natural and anthropogenic sources of bromoform and dibromomethane in the oceanographic and biogeochemical regime of the subtropical North East Atlantic. *Environ. Sci.: Processes Impacts.* **2020**, 22(3), 679-707.
(37) Ulses, C.; Grenz, C.; Marsaleix, P.; Schaaff, E.; Estournel, C.; Meulé, S.; Pinazo, C. Circulation in a semi-enclosed bay under influence of strong freshwater input. *J. Mar. Syst.* **2005***,* 56 (1-2), 113-132.
(38) Millot, C., 1981. Upwelling in the Gulf of Lions. In: Francis, F.A. (Ed.), Coastal Upwelling. American Geophysical Union, Washington, DC. 529 pp.
(39) Estournel, C.; Broche, P.; Marsaleix, P.; Devenon, J.L.; Auclair, F.; Vehil, R. The Rhone River Plume in unsteady conditions: numerical and experimental results. *Estuarine Coastal Shelf Sci*. **2001**, 53 (1), 25-38.
(40) Pacey, N.; Beadle, I.; Heaton, A.; Newsome, L. 2011. Chemical discharges from nuclear power stations: historical releases and implications for Best Available Techniques - Report – SC090012/R1. Environment Agency, Bristol.
(41) Spanel, P. & Smith, D. Selected ion flow tube studies of the reactions of $H_3O$+, NO+, and $O_2^+$ with several aromatic and aliphatic hydrocarbons. *Int. J. Mass Spectrom*. **1999**, 184, 175-181.
(42) Mayhew, C.A.; Thomas, R.; Watts, P. A selected ion flow tube investigation of the positive ion chemistry of a number of bromines containing fully and partially halogenated hydrocarbons. *Int. J. Mass Spectrom*. **2003**, 223-224, 91-105.
(43) Robert-Peillard, F., Palacio Barco, E., Ciulu, M., Demelas, C., Théraulaz, F., Boudenne, J.-L., Coulomb, B., 2017. High throughput determination of ammonium and primary amine compounds in environmental and food samples. *Microchem. J*. **2017**, 133, 216-221.
(44) Ulrich, M.M.; Imboden, D.M.; Schwarzenbach, R.P. MASAS-A user-friendly simulation tool for modelling the fate of anthropogenic substances in lakes. *Environ. Softw.* **1995**, 10, 177-198.

(45) Millero, F.J.; Poisson, A. International one-atmosphere equation of state of seawater. *Deep-Sea Res. Part I-Oceanogr. Res. Pap.* **1981**, 28, 625-629.
(46) Schwarzenbach, R.P.; Gschwend, P. M.; Imboden D.M., 2003. Environmental Organic Chemistry, 2nd edition. Page 1022.
(47) Moore, R.M.; Geen, C.E.; Tait, V.K. Determination of Henry's Law constants for a suite of naturally occurring halogenated methanes in seawater. *Chemosphere* **1995**, *30*, 1183-1191.
(48) Heeb, M.B.; Kristiana, I.; Trogolo, D.; Arey, J.S.; von Gunten, U. Formation and reactivity of inorganic and organic chloramines and bromamines during oxidative water treatment. *Water Res.* **2017**, 110, 91-101.
(49) Criquet, J.; Rodriguez, E.M.; Allard, S.; Wellauer, S.; Salhi, E.; Joll, C.A.; von Gunten, U. Reaction of bromine and chlorine with phenolic compounds and natural organic matter extracts: Electrophilic aromatic substitution and oxidation. *Water Res*. **2015**, 85, 476-486.
(50) Carpenter, L.J.; Jones, C.E.; Dunk, R.M.; K. E. Hornsby, K.E.; Woeltjen, J. Air-sea fluxes of biogenic bromine from the tropical and North Atlantic Ocean. *Atmos. Chem. Phys.* **2009**, 9, 1805-1816.
(51) Butler, J.H.; King, D.B.; Lobert, J.M.; Montzka, S.A.; Yvon-Lewis, S.A.; Hall, B.D.; Warwick, N.J.; Mondeel, D.J.; Aydin, M.; Elkins, J.W. Oceanic distributions and emissions of short-lived halocarbons. *Global Biogeochemical Cycles*, **2007**, 21: GB1023
(52) Fogelqvist, E.; Krysell, M. Naturally and anthropogenically produced bromoform in the Kattegatt, a semi-enclosed oceanic basin. *J. Atmos. Chem.* **1991**, *13(4)*, 315–324.
(53) Petit, J.E.; Favez, O.; Albinet, A.; Canonaco, F. A user-friendly tool for comprehensive evaluation of the geographical origins of atmospheric pollution: wind and trajectory analyses. *Environ. Model. Softw.* **2017**, *88C*, 183-187.
(54) Jenner, H.A.; Taylor, C.J.L.; van Donk, M.; Khalanski, M. Chlorination by-products in chlorinated cooling water of some European coastal power stations. *Mar. Environ. Res.* **1997**, *43(4)*, 279–293.
(55) Allonier, A.S.; Khalanski, M.; Camel, V.; Bermond, A. Characterization of Chlorination By-products in Cooling Effluents of Coastal Nuclear Power Stations. *Mar. Pollut. Bull.* **1999**, *38(12)*, 1232–1241.
(56) Agus, E.; Voutchkov, N.; Sedlak, D.L. Disinfection by-products and their potential impact on the quality of water produced by desalination systems: a literature review. *Desalination* **2009**, *237*, 214-237.
(57) Yang, M.T.; Zhang, X.R. Comparative Developmental Toxicity of New Aromatic Halogenated DBPs in a Chlorinated Saline Sewage Effluent to the Marine Polychaete *Platynereis dumerilii*. *Environ. Sci. Technol.* **2013**, 47, 19, 10868–10876
(58) IARC (International Agency for Research on Cancer). Bromoform. IARC Summary & Evaluation. Vol. 71, **1999**, 1309 p.
(59) US EPA (U.S. Environmental Protection Agency). Integrated Risk Information System (IRIS) on Bromoform. National Center for Environmental Assessment, Office of Research and Development, Washington, D.C. **1999**.
(60) Engel, A. and Rigby, M. (Lead Authors), Burkholder, J. B., Fernandez, R. P., Froidevaux, L., Hall, B. D., Hossaini, R., Saito, T., Vollmer, M. K., and Yao, B.: Update on Ozone-Depleting Substances (ODSs) and Other Gases of Interest to the Montreal Protocol, Chapter 1, in: Scientific Assessment of Ozone Depletion: 2018, Global Ozone Research and Monitoring

Project – ReportNo. 58, World Meteorological Organization, Geneva, Switzerland, 2018.
(61) Sherwen, T.; Schmidt, J.A.; Evans, M.J.; Carpenter, L.J.; Großmann, K.; Eastham, S.D.; Jacob, D.J.; Dix, B.; Koenig, T.K.; Sinreich, R.; Ortega, I.; Volkamer, R.; Saiz-Lopez, A.; Prados-Roman, C.; Mahajan, A.S.; Ordóñez, C. Global impacts of tropospheric halogens (Cl, Br, I) on oxidants and composition in GEOS-Chem. *Atmos. Chem. Phys*. **2016**, 16, 12239-12271.
(62) Mansilha, C.R; Coelho, C.A; Heitor, A.M.; Amado, J.; Martins, J. P., Gameiro, P. Bathing waters: new directive, new standards, new quality approach. *Marine Pollution Bulletin*. 2009,
(63) David, M. Vessels and Ballast Water.' in Matej David and Stephan Gollasch (eds.), Global Maritime Transport and Ballast Water Management - Issues and Solutions (Springer), 2015. Available at: https://link.springer.com/content/pdf/10.1007%2F978-94-017-9367-4.pdf
(64) Jones, E.; Qadir, M.; van Vliet, M.T.H.; Smakhtin, V.; Kang, S.-M. The state of desalination and brine production: A global outlook. *Sci. Total Environ*. **2019**, 657, 1343-1356.